Wideband Fabry-Pérot Resonator for 28 GHz Applications

Ojaroudiparchin, Naser; Shen, Ming; Pedersen, Gert F.

Published in:
Ubiquitous Wireless Broadband (ICUWB), 2016 IEEE International Conference on

DOI (link to publication from Publisher):
10.1109/ICUWB.2016.7790537

Publication date:
2016

Document Version
Early version, also known as pre-print

Wideband Fabry-Pérot Resonator for 28 GHz Applications

Naser Ojaroudi Parchin, Ming Shen, and Gert Frølund Pedersen
Antennas, Propagation, and Radio Networking (APNet) Section
Department of Electronic Systems, Faculty of Engineering and Science
Aalborg University, DK-9220, Aalborg, Denmark
{naser, mish, gfp}@es.aau.dk

***Abstract*—In this paper, a compact design of Fabry-Pérot (FP) resonator for 28 GHz applications is proposed. The antenna is composed of a coaxial-fed source radiator (patch antenna), an air cavity, and a partially reflecting surface (PRS) with 4×4 array of cells. The antenna has a good radiation behavior in the desired operation band of 26–30 GHz with 6 dBi directivity improvement. The antenna is designed on low-cost FR-4 dielectrics (h=0.8 mm, ε=4.3, and δ=0.025). The designed FP resonator exhibits wide bandwidth around 28 GHz which is one the candidate bands for the future fifth generation (5G) wireless systems. It exhibits a high-gain directive-beam pattern in the broadside direction with 12 dBi directivity at 28 GHz. The antenna has a compact size of 25×25 mm^2.**

I. INTRODUCTION

Highly efficient high-gain antennas with single-feed systems such as Reflect-array and Fabry-Pérot (FP) antennas are always desirable as they offer low complexities compared to feeding networks used in conventional antenna arrays [1]. The FP resonator antenna has received intensive attention as an attractive solution to design antennas with high-gain/high-directivity characteristics [2]. A conventional FP antenna is formed by partially reflective surfaces (PRSs), excited by an electromagnetic source located inside or outside the cavity [3]. It has interesting characteristics including low-profile, light weight, high-gain/high-directivity and can be made at low cost.

Our work represents a primarily study on the design and performance of a compact FP resonator antenna which could be used in the future 5G wireless systems [4]. The proposed coaxial-fed FP antenna is achieving a wide bandwidth as well as increased directivity and realized gain. It is designed to work at 28 GHz which is one of the candidate bands of 5G communions [5-7]. An improved design of superstrate for the maximum antenna directivity enhancement is proposed and validated. The proposed FP design consists of a coaxial-fed source radiator excited by a 50 Ohm, an air cavity, and also a PRS which is composed of 4×4 array cells suspended in air at λ/2. The configuration of the unit cell contains a pair of T-shaped slits cut in a square parasitic structure. The proposed antenna obtains more than 12 dBi directivity with wide bandwidth simultaneously. Compared with [8], the proposed design has a compact size while provides wider bandwidth and higher directivities.

II. CONFIGURATION OF THE FP

This work is started by designing a 28 GHz coaxial-fed patch antenna. Then, a PRS superstrate with a 4×4 array of cells is employed above the radiation source. As it is observed in Fig. 1, the distance between the radiation source and the PRS is calculated at d=λ/2 of the resonance frequency (28 GHz). Low-cost FR-4 dielectrics with properties of h=0.8, ε_r= 4.3, and δ=0.025 are used as substrate/superstrate in the proposed structure. The parameter values of the radiation source, PRS and the FP antenna are listed in Table I.

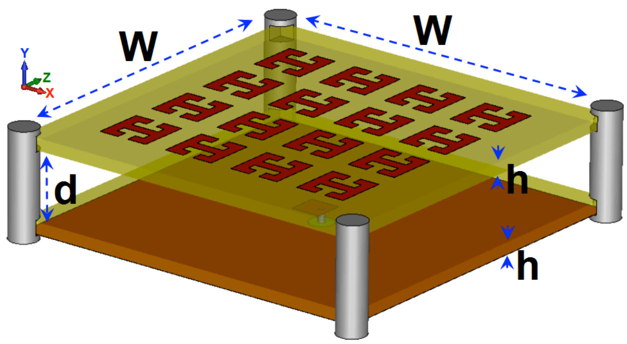

Figure 1. Transparent view of the designed antenna.

TABLE I
DIMENSION VALUES OF THE PROPOSED DESIGN

Parameter	W	W_S	h	W_P	L_P	L_C
Value (mm)	25	5.35	0.8	2.05	2	3
Parameter	r	r_1	r_2	W_U	L_U	W_1
Value (mm)	0.25	0.86	0.9	5.8	11.6	3.5
Parameter	W_T	L_T	W_{T1}	L_{T1}	W_X	d_U
Value (mm)	2	0.75	0.75	0.625	18.5	5

III. 28 GHZ COAXIAL-FED PATCH ANTENNA

Figure 2 displays the configuration of the compact 28 GHz patch antenna. As can be observed, the antenna is fed by a coaxial probe and designed on the FR-4 substrate with compact dimension of λ/2×λ/2. The S_{11} characteristic of the designed patch antenna is depicted in Fig. 3. As illustrated, the antenna has a wide bandwidth (4 GHz) around 28 GHz.

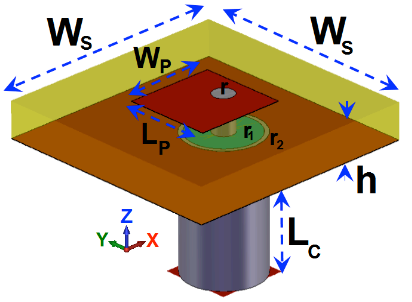

Figure 2. Patch antenna schematic.

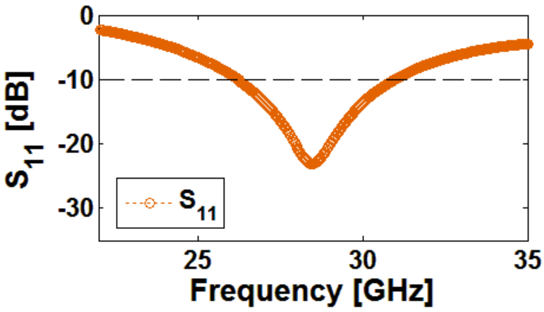

Figure 3. S_{11} of the patch antenna.

The simulated S_{11} characteristics of the patch antenna with different values of W_P&L_P are plotted in Figs. 4 (a) and 4(b), respectively. Based on the obtained results, we can conclude that the antenna operation-band can be controlled by changing the values of the critical parameters such as width and length of the man radiator (W_P&L_P).

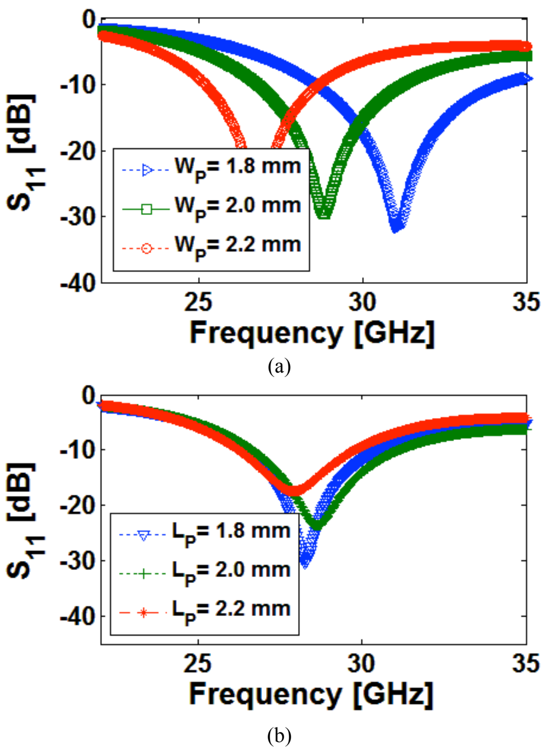

Figure 4. S_{11} characteristics of the antenna for different values of, (a) W_P and (b) L_P.

The simulated radiation pattern of the patch at the resonance frequency (28 GHz) is illustrated in Fig. 5 (a). As seen, the antenna has more than 5.35 dB realized gain with low back lobe. Figure 5 (b) plots the fundamental properties of the antenna behavior in the frequency range of 26 to 30 GHz (operation band). More than 6 dBi directivity with 80% radiation and total efficiencies are achieved for the proposed design. As can be found, the antenna has good and almost constant behavior in its operation band, even though the high-loss FR-4 dielectric is used as the antenna substrate.

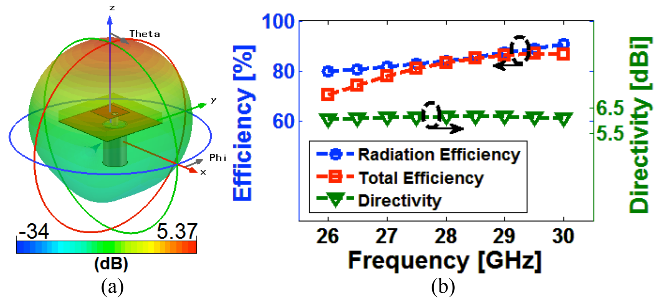

Figure 5. Simulated (a) radiation pattern of the patch antenna at 28 GHz and (b) directivity, radiation and total efficiency characteristics.

IV. The Unit Cell Performance

In this section, the performance of the employed unit cell has been studied. The radiation behavior of the FP resonator highly depends on the performance of the cells used in PRS. The side and top views of the unit cell are shown in Fig. 6. The unit cell configuration is composed of two T-shaped slits inserted in the square parasitic structure. The employed unit cell is designed to work at 28 GHz. However, its operation frequency could be varied by changing the values of the inserted slits. Generally, in order to transmit all energy through the cavity without reflection, the difference between S_{11} and S_{21} coefficients of the unit cells at the operation frequency range must be maximum [9].

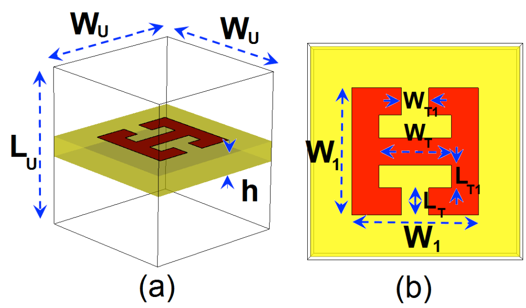

Figure 6. Configuration of the unit cell, (a) side view and (b) top view.

Simulated S_{11} and S_{21} characteristics of the unit cell are plotted in Fig. 7. As can be seen, the designed unit cell has sufficient behavior in the frequency range of 26 to 30 GHz and maximum difference between S_{11} and S_{21} characteristics is obtained. Furthermore, the S_{21} (in phase) characteristic of the unit cell illustrated in Fig. 7, demonstrate the coefficient behavior of the unit cell at 28 GHz.

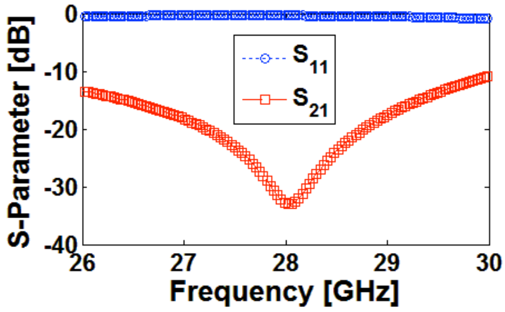

Figure 7. Simulated S_{11} and S_{21} characteristics of the unit cell.

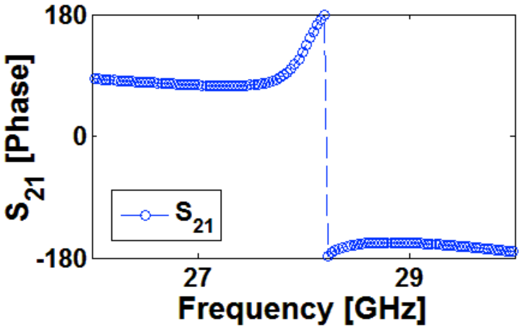

Figure 8. Simulated S_{21} (in phase) for the employed unit cell.

The simulated S_{21} characteristics of the unit cell for different values of the inserted T-shaped slits are represented in Fig. 9. Based on the obtained results, the operation frequency of the unit cell is highly depended on the size of the T-shaped slits and can be tuned for different frequencies.

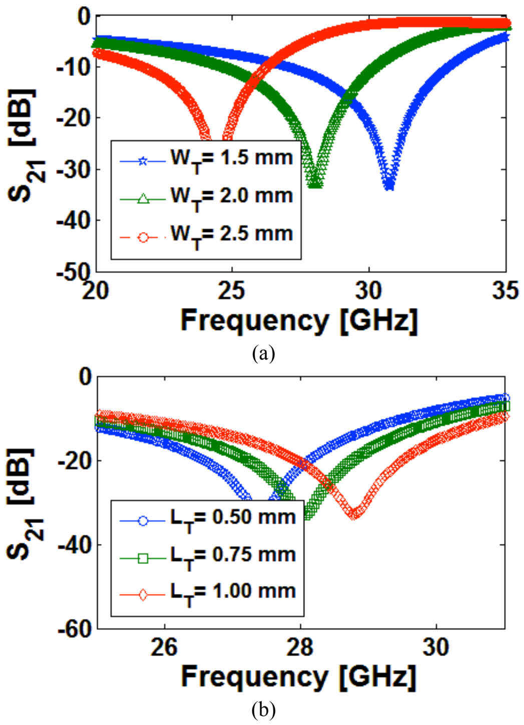

Figure 9. S_{21} characteristics of the unit cell for different values of, (a) W_T and (b) L_T.

Using 4×4 elements of the designed unit cells, a symmetrical PRS superstrate with distance of λ/2 above the radiation source has been designed and employed. Its configuration is shown in Fig. 10. The distance between the cells of PRS is d_U=5 mm.

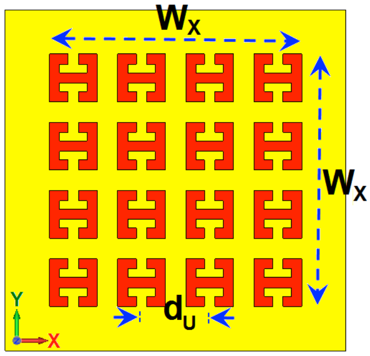

Figure 10. Configuration of the PRS.

V. Radiation Performance of the FP Resonator

In order to demonstrate the effect of the Fabry superstrate on the performance of the radiation source (patch antenna), the current distribution at 28 GHz (resonance frequency) is depicted at Fig. 12. As can be observed, the superstrate has a focusing impact on the distribution of fields in the cavity and can increases the effective aperture area, which leads to improvement of the antenna radiation performance [10].

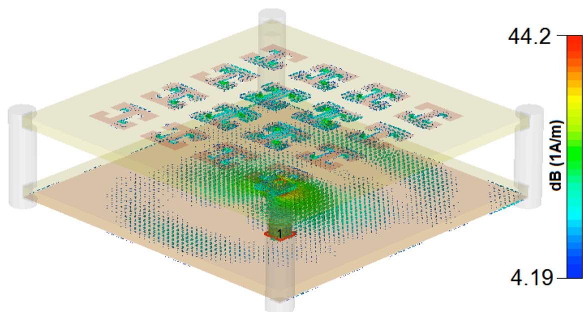

Figure 11. Current distribution of the FP resonator at 28 GHz.

The S_{11} characteristics of the proposed antenna w/wo PRS superstrate are plotted in Fig. 12. Both of the simulated antennas have good frequency responses in the range of 26 to 30 GHz. It can be found that the proposed FP resonator and designed patch antenna have more than 4 GH bandwidth. However there is a discrepancy between their impedance matching characteristics.

In addition, the radiation performance of the antenna w/wo PRS superstae with realized gain values has been investigated. Figure 13 displays 2D-polar radiation characteristics of the antenna w/wo superstrate at the selected frequencies (27, 28, 29 GHz). A significant improvement on the antenna radiation performance with PRS has been achieved. On the other hand, the radiation patterns of the Fabry antenna are more directional compared with basic structure.

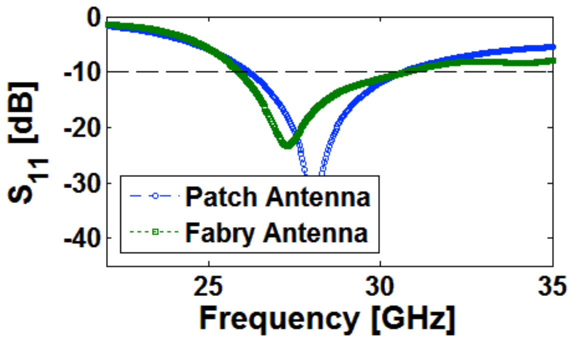

Figure 12. Comparison between the S_{11} characteristics of the basic patch antenna and the proposed FP resonator.

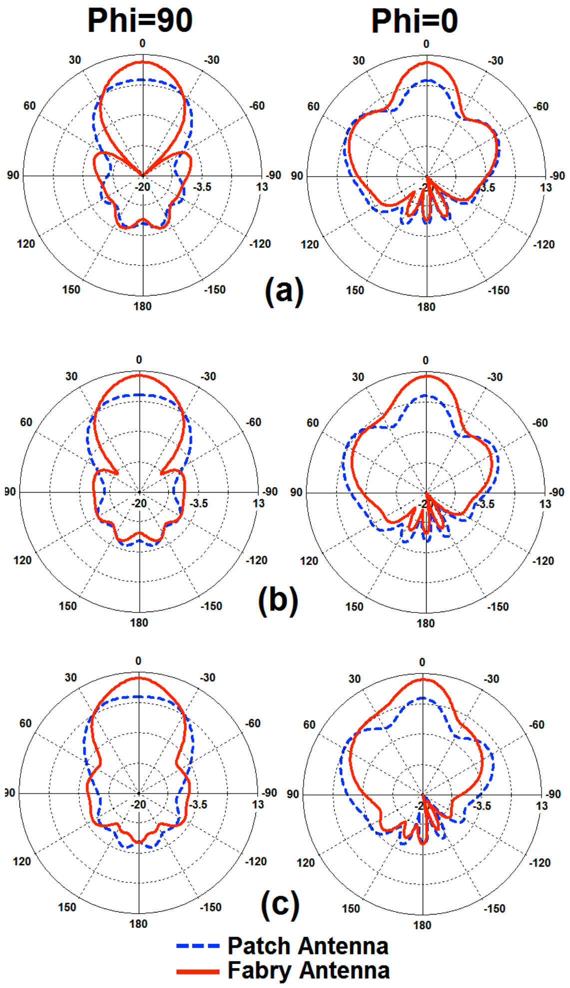

Figure 13. 2D polar radiation patterns of the antenna w/wo superstrate at, (a) 27 GHz, (b) 28 GHz, and (c) 29 GHz.

3D-directional radiation patterns of the antenna with directivity values are displayed in Fig. 14. As seen, the antenna directivity varies from 11.4 to 12.2 dBi in the frequency range of 27 to 29 GHz. In addition, the antenna has good efficiency characteristics (more than 80%) at different frequencies.

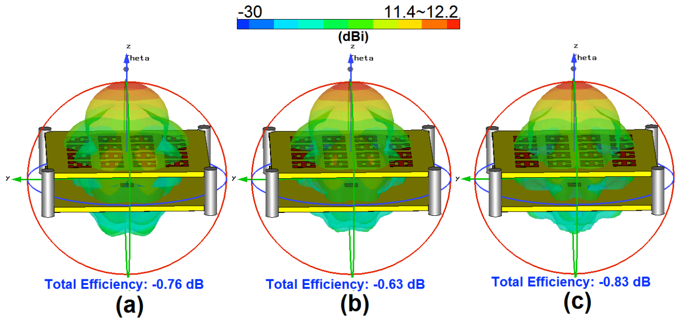

Figure 14. 3D radiation patterns with directivity values at, (a) 27 GHz, (b) 28 GHz, and (c) 29 GHz.

VI. Conclusion

The radiation performance of a FP resonator antenna operating at 28 GHz with high gain and directivity characteristics has been studied. The antenna is excited by coaxial-fed patch with metalized ground plane. The improved directivity function is obtained by utilizing only a single layer of PRS with 4×4 array of cells. The antenna has more than 4 GHz bandwidth with sufficient directivity and efficiency properties. It has good features and could be used as the receiving antenna in the future wireless networks. It also has a compact configuration with easy of fabrication and integration.

References

[1] J. R. Jamesn, P. S. Hall, "*Handbook of microstrip antennas*," Peter Peregrinus Ltd., London, 1989.

[2] H. Boutayeb, *et al.*, "Directivity of an antenna embedded inside a Fabry-Perot cavity: analysis and design," *Microw. Opt. Technol. Lett.*, vol. 48, pp. 12–17, 2006.

[3] K. Lu and K. W. Leung, "Differential Fabry–Perot resonator antennas," *IEEE Transactions on Antennas and Propagation,* vol. 61, pp. 4438-4446, 2013.

[4] Y. Wang, et *al.*, "5G mobile: Spectrum broadening to higher-frequency bands to support high data rates," *IEEE Vehicular Technology Magazine*, vol. 9, pp. 39-46, 2014.

[5] N. Ojaroudiparchin, M. Shen, and G. F. Pedersen, "A 28 GHz FR-4 compatible phased array antenna for 5G mobile phone applications," *International Symposium on Antennas and Propagation* (*ISAP 2015*), November 2015, Australia.

[6] N. Ojaroudiparchin, M. Shen, and G. F. Pedersen, "Design of Vivaldi antenna array with end-fire beam steering function for 5G mobile terminals," *Telecommunications Forum* (*TELFOR 2015*), November 2015, Serbia.

[7] N. Ojaroudiparchin, M. Shen, and G. F. Pedersen, "Multi-layer 5G mobile phone antenna for multi-user MIMO communications," *Telecommunications Forum* (*TELFOR 2015*), November 2015, Serbia.

[8] N. Ojaroudiparchin, M. Shen, and G. F. Pedersen, "Low-profile Fabry-Pérot cavity antenna with metamaterial SRR cells for fifth generation systems," *International Conference on Microwaves, Radar and Wireless Communications (MIKON),* Poland, May 2016.

[9] Z. M. Razi and P. Rezaei, "Multifaceted frequency-selective split ring resonators (SRR)," *IEEE AP-S Int. Symposium on Antennas and Propagation*, July 2012.

[10] Y. Sun, Z. N. Chen, Y. Zhang, H. Chen, and T. S. See, "Subwavelength substrate-integrated Fabry-Pérot cavity antennas using artificial magnetic conductor," *IEEE Transactions on Antennas and Propagation,* vol. 60, pp. 30-35, 2012.